From neutral oligoanilines to polyanilines: A theoretical investigation of the chain-length dependence of the electronic and optical properties

J. Libert, J. Cornil, D. A. dos Santos, and J. L. Brédas
Service de Chimie des Matériaux Nouveaux, Centre de Recherche en Electronique et Photonique Moléculaires, Université de Mons-Hainaut, 20 Place du Parc, B-7000 Mons, Belgium
(Received 13 November 1996)

We investigate theoretically the chain-length dependence of the electronic and optical properties of molecules representative of the three base forms of polyaniline (PAni), i.e., leucoemeraldine, emeraldine, and pernigraniline. The results establish that the PAni oligomers show a weak evolution of their electronic and optical properties as the chain grows, in contrast to the trends observed with other conjugated systems. Such behavior is related to a lack of significant π delocalization of the molecular orbitals, due to the presence along the backbone of nitrogen atoms that interconnect adjacent phenylene rings, and to high-torsion angles induced by steric hindrance between the rings. We also emphasize the need for a correlated approach to properly describe the so-called ''excitonic feature''observed around 2 eV in the optical spectrum of the emeraldine base form. [S0163-1829(97)00837-0]

I. INTRODUCTION

Among conducting polymers, the members of the polyaniline (PAni) family have received considerable attention in the past few years due to their remarkable properties. The generic structural formula of these polymers can be described as

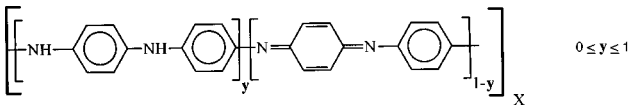

where y corresponds to the ratio within the repeat unit of the number of nitrogen atoms of amine type over the total number of nitrogen atoms. Three distinct pure forms of polyaniline have been experimentally isolated:[1,2]

(i) The fully reduced form ($y=1$) is the leucoemeraldine base [LEB or poly(paraphenylene amine)] which is an insulator [gap of 3.6 eV in *N*-methyl pyrrolidone (NMP) solution[3,4] and 3.8 eV in thin films];[5–7] here, phenylene rings are interconnected by amine nitrogen atoms.

(ii) The half-oxidized form ($y=0.5$) is the emeraldine base [EB or poly(paraphenylene amine imine)] which presents quinoid and aromatic rings in a 1:3 ratio in its chemical structure. The lowest energy absorption feature of this polymer is measured around 2.0 eV in both NMP solution and spin-cast films;[3–7] this peak has often been referred to as an ''excitonic feature'' since the electron transition is believed to be accompanied by a local charge transfer taking place between the quinoid rings and the adjacent aromatic units;[3,8,9] note that the formation of excitons (i.e., bound electron-hole pairs) does not necessarily require local charge transfers to take place in the excited state, as demonstrated for instance by the optical properties of other conjugated oligomers.[10,11] The emeraldine base form also presents a second optical feature at almost the same energy as the absorption peak of the leucoemeraldine base (3.6 eV in NMP solution[3,4] and 3.9 eV in thin films[5–7]).

(iii) The fully oxidized form of polyaniline ($y=0$) is the pernigraniline base [PB or poly(paraphenylene imine)] for which the chemical structure is characterized by an alternation of aromatic and quinoid rings. This polymer has the rare property of possessing a twofold degenerate ground state,[12] as is the case for trans-polyacetylene;[13] the resulting Peierls gap is measured around 2.3 eV, while two other optical features are observed around 3.8 and 4.3 eV in NMP solutions.[14,15]

According to MacDiarmid and co-workers, compounds with intermediate average oxidation levels can be synthesized but actually consist in the mixing of two of the three base forms at the molecular level.[16,17] Indeed, samples with mixed states systematically present the optical properties of both LEB and EB for $y>0.5$ and both EB and PB for $y<0.5$;[16,17] this justifies that in this work we focus our attention exclusively on the three principal base forms.

Polyanilines and derivatives have the peculiarity to present an electrical conductivity that can be controlled either by redox chemistry (i.e., charge-transfer doping)[18] or by Brønsted acid-base chemistry (i.e., protonation).[19,20] In the latter case, it is worth stressing that the electronic structure of the polymer is deeply modified without any alteration of the number of electrons along the chain;[21] the protonation of the imine nitrogen atoms of emeraldine base leads to a dramatic increase in electrical conductivity, up to 12 orders of magnitude (typically from $\sim 10^{-10}$ to ~ 400 S/cm).[22,23] The wealth of the electronic properties of polyanilines makes them good candidates for a wide range of technological applications.[24] Their use in battery devices[25] or in antistatic films[26] has now led to some commercial developments. The conducting properties of emeraldine salts have also allowed for the fabrication of flexible light-emitting diodes where polyaniline is involved as the hole-injecting contact.[27] Note that the electronic properties of polyanilines are controlled both by bond-length dimerization, as in most conjugated polymers, and by torsion-angle dimerization,[28–31] since the phenylene rings leave the plane defined by the nitrogen atoms to reduce the strong sterical hindrance taking place between adjacent rings in the fully planar conformation. These torsions are found to

influence the π delocalization, and hence the mobility of charge carriers along the chains (giving rise to defects with large effective masses when compared to trans-polyacetylene[32,33]) and to deeply affect the electronic properties of polyanilines. Exploitation of these torsional phenomena has recently opened the way to the exploitation of molecular optical memory mechanisms.[34]

For a long time, polyanilines were known as intractable materials, until their solubility in *N*-methylpyrrolidone (NMP) was reported.[35] Meanwhile, studies of oligomer analogs started to emerge as a useful tool to gain insight into the complex properties of the polymers; indeed, low-molecular weight molecules present the advantage of being generally better suited to spectroscopic investigation techniques due to their higher solubility and processibility and their well-defined chemical structure. Despite the fact that polyanilines have attracted a considerable interest, the properties of oligoanilines have been scarcely investigated while an enormous body of knowledge was accumulated for conjugated oligomers such as polyenes, oligo(phenylenevinylene)s, or oligothiophenes.

The first model molecule to be synthesized and characterized was the phenyl-capped octaaniline in its three basic oxidation states;[36] absorption spectra of additional compounds representative of LEB were also subsequently reported.[4,37–39] These studies indicate that the lowest-energy transition of these oligomers is observed at almost the same energy as in the corresponding polymer. Regarding earlier theoretical modeling carried out on oligoanilines, to the best of our knowledge, only calculations based on a modified neglect of differential overlap (MNDO) geometry optimizations coupled to intermediate neglect of differential overlap/configuration interaction (INDO/CI) optical calculations have been reported for tetramers representative of the three base forms of polyaniline.[40] Note that Hartree-Fock-Austin model 1 (AM1) optimizations of short LEB (dimer, tetramer, and pentamer) and PB (trimers) neutral oligomers have also been presented in two of our previous studies; in contrast, one-electron band structures of polyanilines have received much more attention.[28,31,41]

In this work, we investigate the electronic and UV-visible optical properties of oligomers and corresponding polymers representative of the three base forms of polyaniline by means of quantum-chemical methods. We particularly pay attention to the chain-length evolution of these properties and analyze the extent to which the results obtained with oligoanilines can be extrapolated to the polymer scale.

We structure the present paper as follows: we treat in a separate way the series of oligomers representative of the same base form of polyaniline. In each case, we first focus on the description of the AM1-optimized geometry of the unit cell, which is directly extracted from the center of the longest oligomers. We then discuss the valence effective Hamiltonian (VEH) and INDO/SCI-calculated optical properties of the oligoanilines and compare these results to previous experimental and theoretical studies. Finally, the VEH polymer band structures and related absorption spectra are presented; it has to be emphasized that the VEH band structures have already been reported in earlier publications[30,42] and that the purpose of discussing them here again is to assess the validity of a one-electron picture, by critically comparing the VEH data to the results of our correlated calculations. In this way, this work should contribute to a refined description of the electronic and optical properties of the three neutral base forms of PAni.

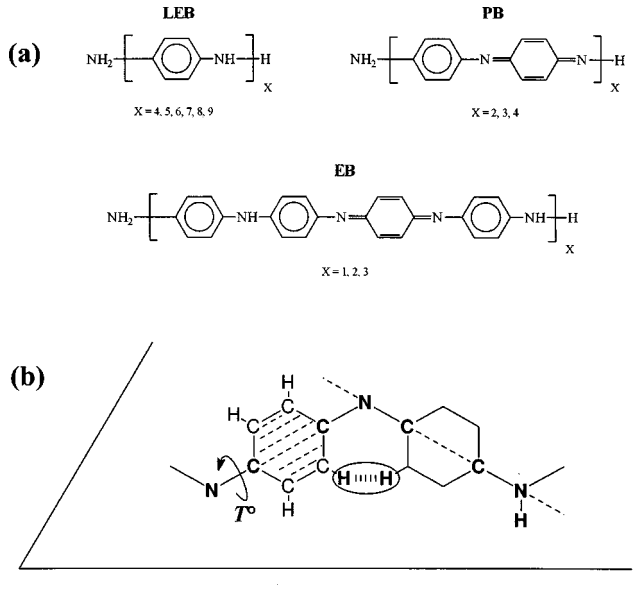

FIG. 1. (a) Chemical structure of the PAni oligomers investigated in this work; (b) sketch of the geometric constraints imposed during the geometry optimizations.

II. THEORETICAL METHODOLOGY

We review in Fig. 1(a) the chemical structure of the PAni oligomers investigated in this work that are systematically capped by $-NH_2$ terminal groups. In a first stage, we optimize the geometry of the molecules by means of the semiempirical Hartree-Fock-Austin model 1 (AM1) method,[43,44] known for its good track record to reproduce accurately the geometry and heat of formation of organic compounds in their ground state. We stress that the AM1 parametrization is particularly convenient to deal with systems where torsional aspects play a significant role; the applicability of this method to the study of polyanilines has been addressed in earlier works.[30,42] The optimization procedure is performed by setting the nitrogen atoms and the para carbon atoms of the rings in the same plane (as suggested by x-ray-diffraction experiments[37,45]), and by imposing the coplanarity of the carbon atoms of the phenylene rings and the sp^2 character of the nitrogens; these geometric constraints are sketched in Fig. 1(b). The torsion angle of a phenylene ring is defined in the following as the dihedral angle between the plane of the nitrogen atoms and the plane of the ring.

On the basis of the optimized geometric structures, the electronic transition energies of the PAni oligomers and related oscillator strengths are calculated by means of:

(i) the pseudopotential one-electron valence effective Hamiltonian (VEH) technique,[46,47] as implemented by Stafström and Brédas.[41]

(ii) the semiempirical Hartree-Fock intermediate neglect of differential overlap (INDO) method coupled to a single configuration interaction scheme (SCI).[48] The electron-electron repulsion terms are calculated via the Mataga-Nishimoto potential that is best suited to reproduce the

optical-absorption spectra of neutral compounds within the INDO/SCI formalism. The number of configurations involved in the CI calculations is chosen in a way that ensures that no significant changes in the transition energies and transition moments occur when considering additional configurations; our CI development is based on singly excited configurations generated by the promotion of an electron from one of the 35 highest occupied levels to one of the 35 lowest unoccupied levels. Note that all the theoretical absorption spectra presented in this paper are simulated by a convolution of Gaussians whose full width at half maximum is set to 0.3 eV.

In a last step, we determine the VEH one-electron band structure of the polymers and the associated absorption spectra,[46,47] on the basis of a repeat unit extracted from the AM1-optimized geometry of a corresponding oligomer. These calculations allow us to estimate accurately the electronic parameters (such as ionization potential, electron affinity, band gap, and bandwidths) that govern the electronic and optical properties of single polyaniline chains. Note that the VEH parameters involved in the definition of the atomic potentials are of similar quality as those provided by *ab initio* Hartree-Fock double zeta calculations; the reliability of this method to reproduce the band structure of conjugated polymers has been widely recognized in earlier works.[31,49]

III. RESULTS AND DISCUSSION

A. Leucoemeraldine base

1. Geometric structure

The AM1-optimized geometry of the unit cell representative of LEB, as extracted from the center of the nonamer, is reported in Fig. 2(a). As previously reported,[30,42] we observe that the phenylene rings present an aromatic character and leave the plane defined by the nitrogen atoms with an alternating torsion angle of $\pm 28°$; therefore, the leucoemeraldine chains display no dimerization for bond lengths and for torsion angles.

2. VEH oligomer calculations

The most significant linear combination of atomic orbitals (LCAO) coefficients of the highest occupied molecular orbital (HOMO) and lowest unoccupied molecular orbital (LUMO) levels are systematically localized on the inner part of the molecule (involving for instance, about five phenylene rings and six nitrogens in the nonamer). The amplitude of these wave functions is maximal in the center of the oligomer and decreases when moving to its extremities; however, these wave functions become much more uniform (with a simultaneous decrease in intensity for the LCAO coefficients) and extended in the inner part of the oligomer when the molecular size is increased. The spatial evolution of the HOMO and LUMO wave functions with increasing chain length therefore points out the existence of a continuous transition in the electronic properties when going from the LEB oligomers to the corresponding polymer. The wave functions of the HOMO and LUMO levels of the oligomers are found to markedly differ due to a breakdown of the electron-hole symmetry induced by the incorporation of nitrogen atoms

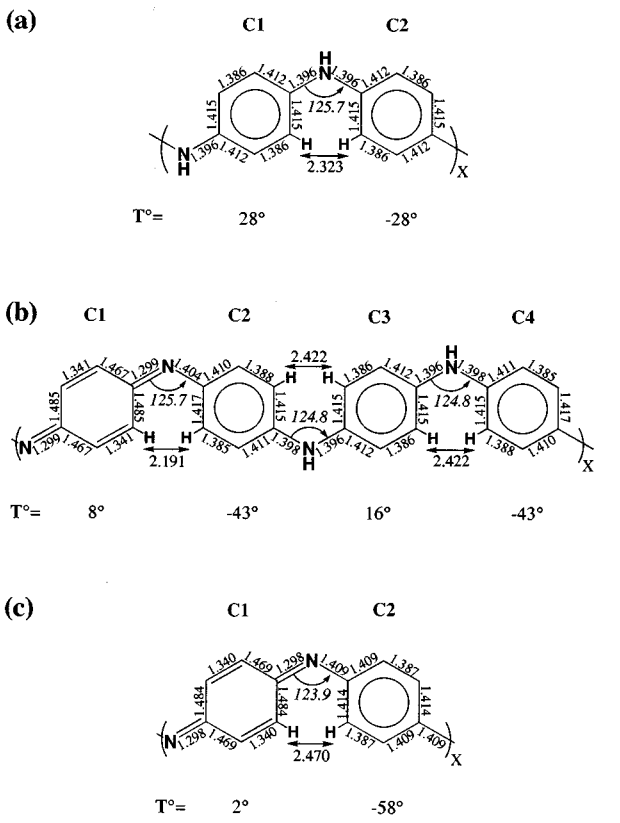

FIG. 2. AM1-optimized geometry of (a) LEB; (b) EB; and (c) PB unit cells. The bond lengths and the distance between interacting hydrogens are in Å, while the bond angles and the torsion angles (T) are in degrees.

along the backbone; this behavior has already been described in detail for the leucoemeraldine base in a previous study.[42]

In the VEH-calculated absorption spectra of the LEB oligomers [see Fig. 3(a)], a broad feature is observed in the energy range between 3.6 and 5.0 eV. The peak maximum position is found to slightly redshift with increasing chain length and to saturate rapidly in the longer oligomers (from 4.40 for the tetramer to 4.18 eV for the octamer and nonamer), as is the case for the VEH-calculated HOMO→LUMO ($H \rightarrow L$) transition (calculated at 4.01, 3.97, 3.93, 3.90, 3.89, and 3.87 eV in LEB oligomers containing 4, 5, 6, 7, 8, and 9 phenylene rings, respectively). Such an evolution clearly demonstrates the existence of a small bathochromic shift of the lowest energy transition as the chain grows. Extrapolation of the $H \rightarrow L$ transition energy to the polymer scale leads to a value for the LEB band gap close to 3.8 eV, in close agreement with the value provided by a previous study on phenyl-capped LEB oligomers.[42] Many electronic excitations involving the upper occupied and lower unoccupied levels contribute to the broad absorption band observed between 3.6 and 5.0 eV; all these transitions involve levels close in energy [as shown in Fig. 4(a), for the LEB nonamer] giving rise to the formation of the valence and conduction bands at the polymer scale.

3. INDO/SCI calculations

We provide in Table I a detailed description of the nature of the INDO/SCI absorption features calculated below 4.0

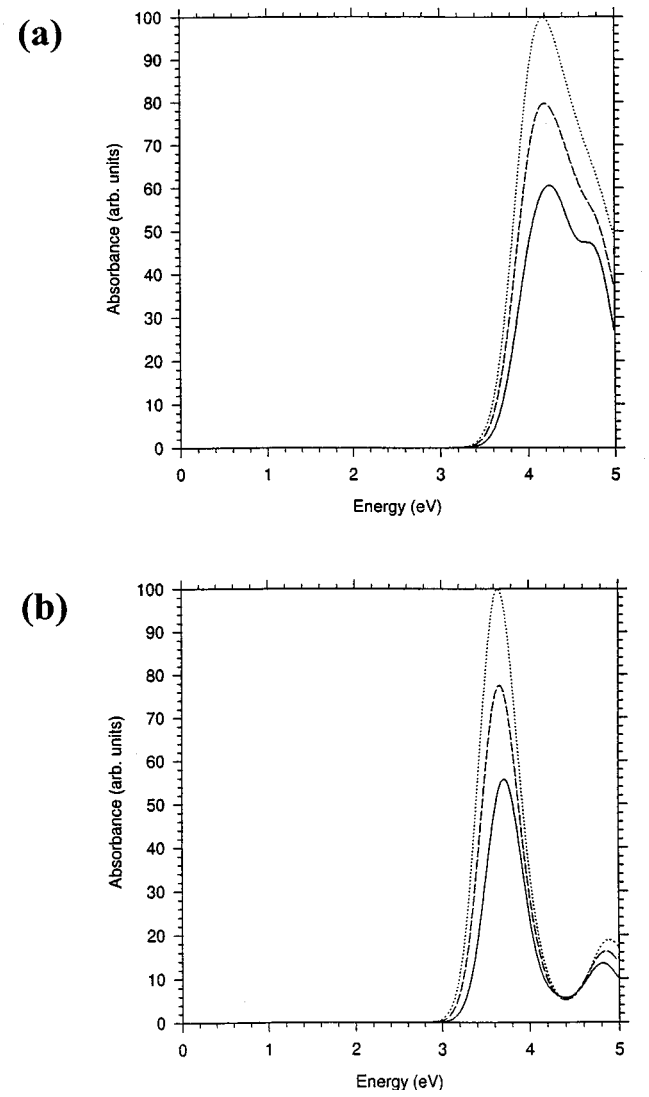

FIG. 3. (a) VEH and (b) INDO/SCI calculated absorption spectra of the five- (solid line), seven- (dashed line), and nine-ring (dotted line) LEB oligomers.

eV in the five-, seven-, and nine-ring LEB oligomers. The results indicate that the lowest energy absorption feature is the most intense and mainly corresponds to an electron transition between the HOMO and LUMO levels, with minor contributions arising from the $H-1 \rightarrow L+1$ and $H-2 \rightarrow L+2$ excitations, especially in longer chains. We further note that the CI expansion coefficient associated with the $H \rightarrow L$ configuration diminishes with increasing chain length, as is typically found in other conjugated oligomers.[50] The INDO/SCI results also indicate the existence of additional calculated features between 3.75 and 3.93 eV, for which the largest CI expansion coefficient is associated with electron transitions between the highest last occupied levels (HOMO, H-1 and H-2) and lowest unoccupied levels above the LUMO (see Table I). However, the relative intensities of these features are attenuated with increasing chain length so that the first peak is the dominant band in the absorption spectra of the longest chains. We display in Fig. 3(b) the simulated optical-absorption spectra of the five-, seven-, and nine-ring LEB oligomers; these plots illustrate the existence of a small bathochromic shift of the lowest energy transition, as observed within the VEH formalism, and indicate that the intensity of this absorption band increases almost linearly with molecular size. We note that similar trends are obtained for the four-, six-, and eight-ring LEB oligomers. The fact that the first absorption peak [see Fig. 3(b)] corresponds to a vast mixing of one-electron excitations for long oligomers illustrates that the corresponding compounds can be described in terms of bands rather than discrete molecular levels.

The weakness of the lowest transition redshift (going from 3.69 to 3.61 eV within the series of oligomer we have considered, see Table I) is in marked contrast with the typical optical properties observed in oligomers representative of common conjugated polymers.[50–55] This behavior is related to the high torsion angles between rings in LEB, that limit the degree of delocalization of the HOMO and LUMO wave functions, and to the presence of nodes on nitrogen atoms that prevents the wave functions of the LUMO and higher unoccupied molecular orbitals to be fully delocalized.[42] As a consequence, the calculated transition energies obtained for the oligomers are in excellent agreement with the 3.8 eV reported for LEB thin films[3,4] (while 3.6 eV is measured in NMP solution[5–7]).

Our theoretical INDO/SCI results are consistent with the experimental absorption spectra of LEB oligomers; the lowest energy transition of N,N'-diphenylphenylenediamine is indeed measured around 3.8 eV in NMP solution,[37] while 4.0 eV is obtained for the phenyl-capped tetramer in acetonitrile solution.[4] The INDO/SDCI calculations performed by

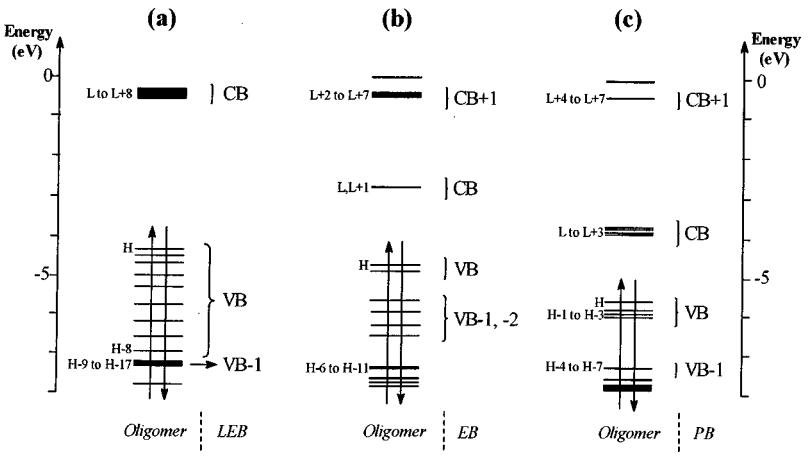

FIG. 4. VEH-calculated one-electron structure of the (a) nine-ring LEB, (b) eight-ring EB, and (c) eight-ring PB oligomers.

TABLE I. INDO/SCI transition energies, oscillator strengths, and main CI expansion coefficients of the lowest energy absorption features (below 4.0 eV) in the LEB oligomers (H and L refer to the HOMO and LUMO levels, respectively).

Number of rings	Transition energy (eV)	Oscillator strength	Main CI expansion coefficients of the excited states
5	3.69	1.50	$0.80(H\rightarrow L)-0.43(H-1\rightarrow L+1)$
	3.77	0.34	$-0.69(H\rightarrow L+2)-0.33(H-1\rightarrow L+3)$ $+0.26(H-2\rightarrow L+4)$
	3.92	0.17	$-0.57(H\rightarrow L+6)-0.48(H-1\rightarrow L+5)$ $-0.34(H-2\rightarrow L+4)$ $-0.27(H-3\rightarrow L+3)$
7	3.63	2.27	$-0.72(H\rightarrow L)+0.45(H-1\rightarrow L+1)$ $-0.31(H-2\rightarrow L+3)$
	3.75	0.32	$0.63(H\rightarrow L+2)+0.36(H-1\rightarrow L+4)$ $-0.27(H-2\rightarrow L+5)$
	3.93	0.23	$-0.48(H\rightarrow L+10)-0.46(H-1\rightarrow L+8)$ $+0.38(H-2\rightarrow L+7)$ $-0.29(H-3\rightarrow L+6)$
9	3.61	2.96	$0.66(\mathrm{H}\rightarrow\mathrm{L})-0.44(\mathrm{H}-1\rightarrow\mathrm{L}+1)$ $-0.34(H-2\rightarrow L+2)$
	3.75	0.36	$0.57(\mathrm{H}\rightarrow\mathrm{L}+3)+0.35(\mathrm{H}-1\rightarrow\mathrm{L}+4)$ $-0.28(H-2\rightarrow L+5)$
	3.92	0.28	$-0.46(\mathrm{H}\rightarrow\mathrm{L}+2)+0.40(\mathrm{H}-2\rightarrow\mathrm{L})$ $-0.36(H-1\rightarrow L+1)$
	3.93	0.28	$-0.43(\mathrm{H}-1\rightarrow\mathrm{L}+12)+0.41(\mathrm{H}\rightarrow\mathrm{L}+13)$ $+0.37(H-2\rightarrow L+10)$ $-0.32(H-3\rightarrow L+9)-0.25(H-4\rightarrow L+8)$

Sjögren and Stafström on the LEB tetramer capped by a single $-NH_2$ terminal group[40] estimate the lowest transition energy at 3.95 eV. Surprisingly, the nature of the lowest-lying excited state they calculate with their INDO parametrization corresponds to a large mixing of one-electron excitations instead of the dominant contribution of the HOMO-LUMO transition, we find in our case. We have investigated the influence of amino terminal groups ($-NH_2$) on the optical properties of LEB oligomers; they have actually negligible effects on the transition energies, due to the absence of significant LCAO coefficients on these sites in the wave functions of the levels involved in the description of the peaks. It must be emphasized that the INDO/CI results obtained by Stafström and Sjögren on the aniline oligomers have to be regarded with much caution due to parametrization problems.[56]

4. VEH band structure

We reproduce in Fig. 5(a) the one-electron band structure of the neutral leucoemeraldine base that we detailed previously.[42] Due to the glide-plane symmetry within the unit cell of the polymer [see Fig. 2(a)], the bands are degenerate at the end of the Brillouin zone ($k=\pi/a$). The valence (HOMO) and conduction (LUMO) bands are characterized by large (2.81 eV) and flat (0.17 eV) bandwidths, respectively; these bands are separated by a band-gap value of 3.81 eV that compares very well to the experimental transition energy,[3] as well as to the VEH and INDO/SCI results obtained for the LEB oligomers. This validates the choice of the one-electron VEH approach to estimate the lowest energy transition of leucoemeraldine base. The calculated ionization potential and electron affinity, corrected for solid-state effects, are estimated to be 4.3 and -0.5 eV, respectively. The very small electron affinity of the polymer indicates that LEB films should not be easily reduced.

The polymer VEH absorption spectrum of LEB is presented in Fig. 5(b). The electronic transition peaking at 4.03 eV is found to dominate the spectrum, while a second less intense feature is observed around 4.90 eV. The broad band lying between 3.6 and 5.0 eV actually originates from one-electron transitions between the valence and conduction bands, covering the impulsion range going from $k=0$ (band gap $E_g=3.81$ eV) to $k=\pi/a$ ($E_g=4.99$ eV), although the most intense excitations involve electronic transitions occurring near $k=0$.

As illustrated in Fig. 6(a),[42] the analysis of the VEH-LCAO-π coefficients of the frontier bands of the LEB unit cell have revealed a strong breakdown of charge conjugation symmetry since the HOMO is delocalized over the whole unit cell, while the LUMO is essentially localized within the phenylene rings.[42]

B. Emeraldine base

1. Geometric structure

We illustrate in Fig. 2(b) the AM1-optimized geometry of the EB unit cell, as extracted from the center of the 12-ring oligomer (i.e., the EB trimer). The repeat unit is composed by three consecutive phenylene rings ($C2$, $C3$, and $C4$) that present an aromatic character ($C_p-N\sim1.399$ Å, C_p-C_o

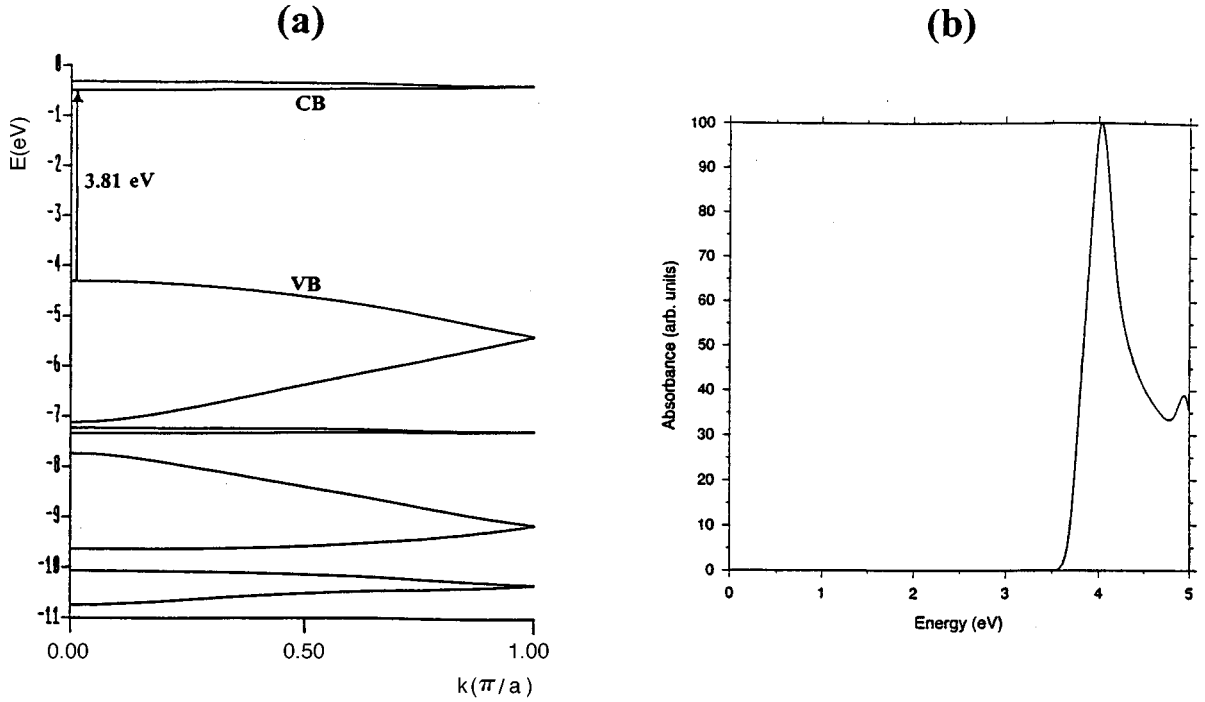

FIG. 5. VEH results relative to a neutral single LEB chain: (a) calculated one-electron band structure; (b) associated optical-absorption spectrum.

$\sim$1.413 Å, and $C_o-C_o\sim$1.386 Å, where *p* and *o* denote the para and ortho positions, respectively) and by a fourth ring adopting a quinoid character ($C_p-N=1.299$ Å, $C_p-C_o\sim1.476$ Å, and $C_o-C_o=1.341$ Å). Analysis of the optimized torsion angles indicates that the quinoid ring slightly leaves the plane defined by the nitrogen atoms ($T=8°$), while the adjacent rings largely go out of this plane ($T=-43°$) in order to minimize the steric hindrance; the departure of planarity of the central aromatic ring ($C3$) is then not as large ($T=16°$) due to the fact that high torsion angles are found for the adjacent two aromatic rings. We note that the optimized geometry provides a value close to 59° for the dihedral angle between adjacent aromatic rings that is almost identical to the angle obtained for the LEB chains (56°). The aromatic part of the EB unit cell can thus be considered to correspond to a LEB segment, still characterized by the absence of bond-length dimerization; however, we observe the appearance of a torsion-angle dimerization ($\Delta T\approx29°$) between the aromatic rings due to the introduction of quinoid moieties that impose new steric constraints along the chain. The EB chain can thus be described as an array of LEB trimerlike units interconnected by quinoid moieties, i.e., an alternated ''copolymer'' of LEB and PB.

2. VEH oligomer calculations

In the EB dimer (H_2N—*AQAAAQAA*—NH_2, where *A* and *Q* denote aromatic and quinoid rings, respectively), the HOMO and HOMO-1 wave functions are mostly localized on the central part of the aromatic segments. Due to their similarity, these two levels are close in energy [-4.71 and -4.85 eV, respectively; see Fig. 4(b)]. Furthermore, we note that the HOMO-2 (-5.56 eV) and HOMO-3 (-5.84 eV) levels also present similar wave functions (localized on the imine units and on the adjacent aromatic rings), and possess similar energies. These results again illustrate that the electronic bands progressively build up as the chain grows [see Fig. 4(b)]. The LUMO (-3.77 eV) and LUMO+1 (-3.74 eV) levels are also almost degenerate and centered on the imine-quinoid segments. This analysis confirms that the HOMO and LUMO levels of EB have the same electronic characteristics as in the LEB and PB (see below) oligomers, respectively; this validates the description of EB in terms of an alternated ''copolymer'' of LEB and PB.

The VEH-calculated absorption spectra of the EB monomer, dimer, and trimer are collected in Fig. 7(a): there occurs three peaks below 4.0 eV for each compound; in the case of the dimer (eight-ring oligomer), the peaks appear at 0.97, 1.83, and $\sim$2.60 eV and correspond to $H\rightarrow L$ (for the most intense transition), $H-2\rightarrow L+1$, and $H-4,-5\rightarrow L$ electronic transitions, respectively. We also observe an intense peak around 4.2 eV that originates from the overlap of electronic transitions involving a large set of occupied and unoccupied levels. It is worth stressing that these results fail to rationalize the experimental measurements where a single, strong peak, often referred to as an ''excitonic feature'', is observed at $\sim$2.0 eV.[3] This failure is attributed to the one-electron nature of the VEH approach as demonstrated in the next section.

3. INDO/SCI calculations

The INDO/SCI calculations result in two dominant absorption features at 2.59 and 3.64 eV in the optical-absorption spectrum of the EB dimer [see Fig. 7(b)]. The lowest absorption peak actually originates in the superimposition of two transitions, at 2.58 and 2.64 eV, that present relative intensities in a 7:1 ratio, as reported in Table II; the main contribution to the total intensity is thus given by the lowest energy transition that involves the *H* and *H*-2 levels

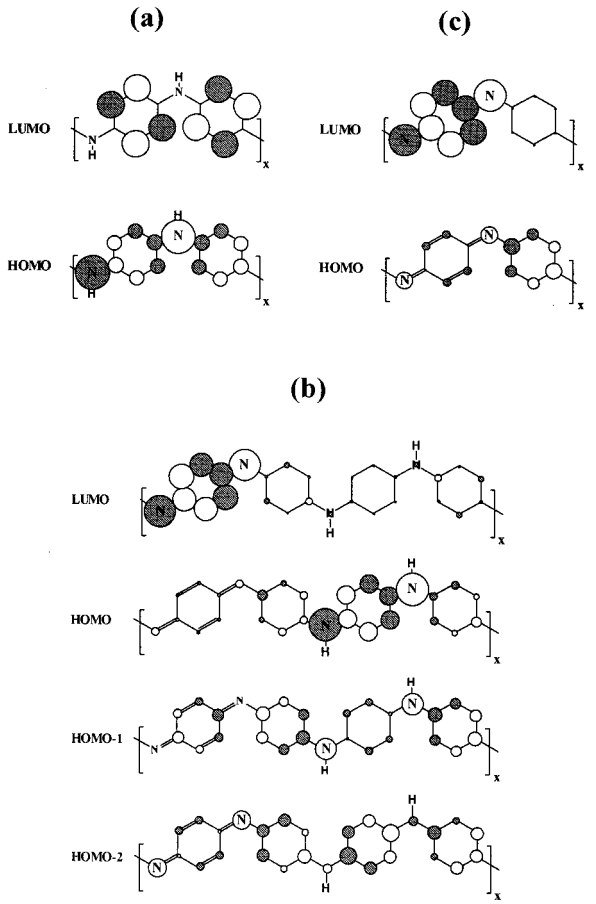

FIG. 6. Illustrations of the VEH-LCAO-π coefficients of the frontier bands of (a) LEB; (b) EB; and (c) PB.

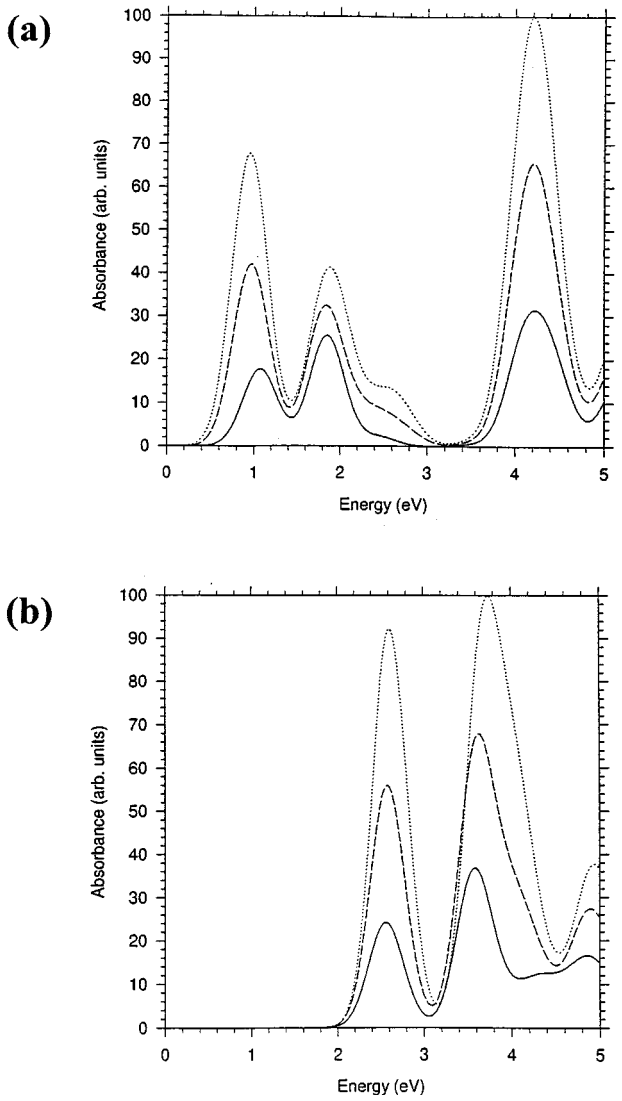

FIG. 7. (a) VEH and (b) INDO/SCI calculated absorption spectra of the EB monomer (solid line), dimer (dashed line), and trimer (dotted line).

and the lowest two unoccupied levels. The second absorption peak calculated around 3.6 eV results from the superimposition of three optical transitions that are all described by a large mixing of configurations involving deep occupied levels and the lowest three unoccupied molecular orbitals. We emphasize that the changes in charge distributions, when going from the ground state to the lowest-lying singlet excited state, take place from two ═N—*A*—NH— units (loss of $-0.23|e|$ for each) to the quinoid ring they surround (gain of $-0.46|e|$). We thus expect a strongly confined intramolecular charge-transfer (in the sense that a local charge transfer is observed between different units of the chain) exciton to be generated upon photoexcitation. Similar results have been obtained for the monomer in which a charge transfer of $-0.50|e|$ is calculated.

The INDO/SCI results are in good agreement with the experimental transition energies of the octamer[36] and the polymer,[3–7] which are measured around 2.0 and 3.8 eV; our results therefore stress the need for a correlated approach in order to describe properly the 2.0 eV absorption feature of EB. However, the INDO/SCI calculations are found to overestimate by ~ 0.6 eV the experimental value reported for the lowest transition energy. This shift can be partly attributed to polarization effects induced by polar environment (such as a NMP solution) that could stabilize the charge-transfer lowest excited state; such environmental effects have not been taken into account in the present calculations. We also mention that our INDO/SCI approach simply deals with vertical transition energies; the lattice relaxation occurring in the lowest-lying singlet excited state (i.e., the ''excitonic'' state) is thus not addressed. Direct AM1/SCI optimization of this excited state actually depicts the charge transfer in a slightly different manner than the INDO/SCI calculations, namely by a local charge transfer of about $-0.50\ |e|$ taking place from the —*A*—NH—*A*— sites to the quinoid sites (—N═*Q*═N—), i.e., from the reduced units to the oxidized units.

The theoretical results obtained for the EB monomer and trimer are very similar to those reported for the dimer. Going from the monomer to the trimer, it is interesting to observe in Fig. 7(b) that the first absorption peak position remains almost unchanged (~ 2.60 eV), while the second absorption band is slightly blueshifted (from 3.59 to 3.74 eV), both intensities increasing significantly with the oligomer size. We should thus keep in mind that EB oligomers are also characterized by a lack of significant evolution of their opti-

TABLE II. INDO/SCI transition energies, oscillator strengths, and main CI expansion coefficients of the lowest energy absorption features (below 4.5 eV) in the EB oligomers.

Number of rings	Transition energy (eV)	Oscillator strength	Main CI expansion coefficients of the excited states
4	2.56	0.76	$-0.59(H\rightarrow L)-0.59(H-1\rightarrow L)-0.30(H-8\rightarrow L)$
	3.57	1.12	$-0.49(H-8\rightarrow L)+0.40(H-4\rightarrow L)+0.38(H\rightarrow L)$
	4.21	0.19	$0.58(H\rightarrow L+1)+0.40(H\rightarrow L+4)-0.33(H\rightarrow L)$ $+0.29(H\rightarrow L+5)$
8	2.58	1.56	$0.60(H-2\rightarrow L+1)+0.36(H\rightarrow L+1)$ $+0.35(H\rightarrow L)$
	2.64	0.22	$-0.41(H\rightarrow L)-0.38(H-1\rightarrow L)+0.37(H-3\rightarrow L)$ $+0.30(H-2\rightarrow L)$ $+0.30(H\rightarrow L+1)$
	3.59	1.85	$-0.35(\mathrm{H}\rightarrow\mathrm{L})+0.28(\mathrm{H}-10\rightarrow\mathrm{L})$ $+0.27(H-15\rightarrow L+1)$ $-0.26(H\rightarrow L+2)$
	3.77	0.17	$-0.55(H-1\rightarrow L)+0.28(H\rightarrow L)+0.21(H\rightarrow L+2)$
	3.86	0.19	$0.51(\mathrm{H}-2\rightarrow\mathrm{L}+1)-0.47(\mathrm{H}\rightarrow\mathrm{L}+1)$ $-0.29(H-14\rightarrow L+1)$ $-0.25(H-15\rightarrow L+1)$
	4.09	0.44	$-0.59(H-3\rightarrow L)-0.46(H\rightarrow L)+0.32(H-4\rightarrow L)$
	4.27	0.20	$0.37(\mathrm{H}-1\rightarrow\mathrm{L}+2)+0.30(\mathrm{H}-1\rightarrow\mathrm{L}+3)$ $+0.29(H-1\rightarrow L)$ $+0.27(H-1\rightarrow L+11)-0.25(H-1\rightarrow L+8)$

cal properties as a function of chain size. We finally note that a detailed comparison with the previous theoretical results reported by Sjögren and Stafström[40] based on different parametrization and geometric structure appears rather difficult.

4. VEH band structure

On the basis of the AM1-optimized geometry of the unit cell [Fig. 2(b)], we have calculated the one-electron band structure of a single emeraldine base chain, see Fig. 8(a)

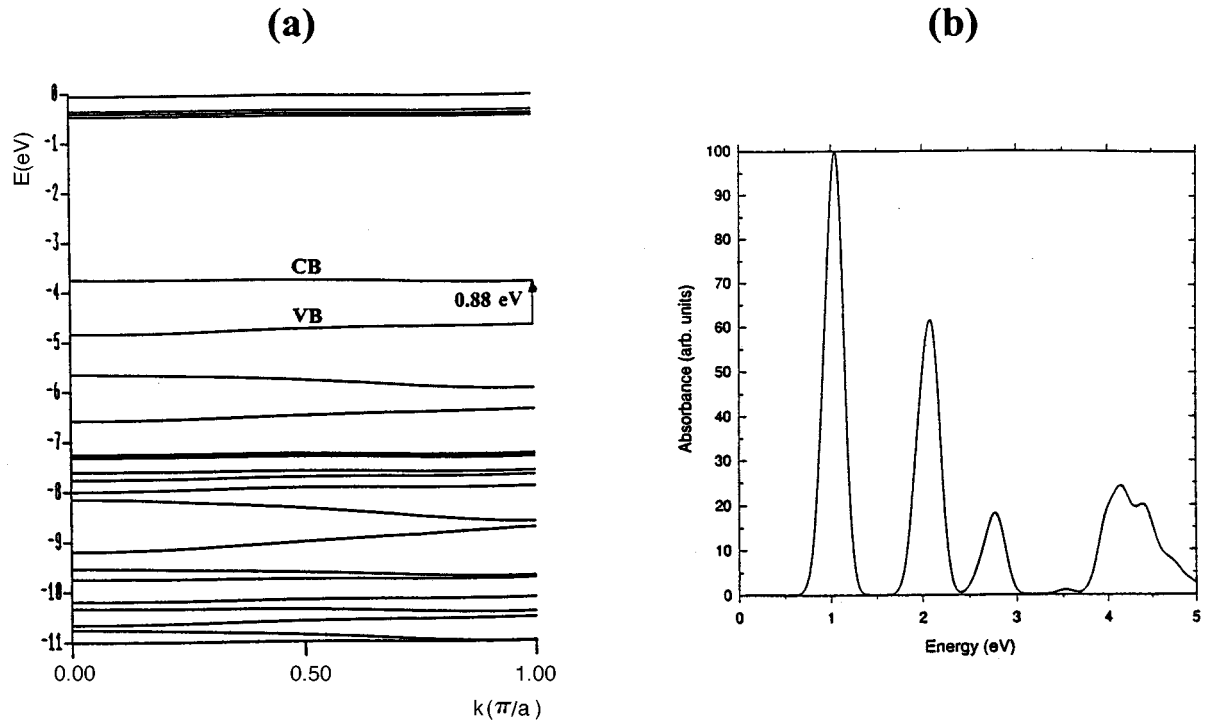

FIG. 8. VEH results relative to a neutral single EB chain: (a) calculated one-electron band structure; (b) associated optical-absorption spectrum.

(note that there are twice as many bands as in the LEB band structure since the size of the EB unit cell is twice as large as that of LEB). The loss of the glide-plane symmetry makes the valence band of LEB split into four narrow bands, the highest of them constituting the conduction band of the EB chain.[31] The valence band and the conduction band are separated by a band-gap value of 0.88 eV. The values of the ionization potential and electron affinity, corrected for solid-state effects, are calculated to be 4.7 and -3.8 eV and are intermediate with regard to those calculated for LEB and PB (see below).

The VEH absorption spectrum of the EB polymer presented in Fig. 8(b) is in deep contrast with the experimental spectrum, where a single intense peak is observed at ~ 2.0 eV.[3] This discrepancy was expected since the INDO/SCI calculations have demonstrated that a correlated approach is required to describe the absorption spectrum in EB chains. However, it is worth stressing that the EB valence density of states spectrum calculated on the basis of the VEH band structure matches well recent ultraviolet photoelectron spectroscopy (UPS) data;[57] this confirms that the one-electron structure is well reproduced within the VEH formalism.

The VEH-LCAO-π coefficients of the HOMO, H-1, H-2, and LUMO of the EB unit cell are presented in Fig. 6(b). The wave function of the HOMO is mainly localized on the amine units and the aromatic ring they surround. The wave function of the H-1 level extends chiefly on the amine sites and on all the phenylene rings. In contrast, the H-2 wave function presents its largest contributions on the imine sites and all the aromatic rings. We finally note that the LUMO is mainly localized on the quinoid ring and the imine sites while the $L+1$ is essentially localized within the phenylene rings, as observed in LEB [see the LUMO description in Fig. 6(a)].

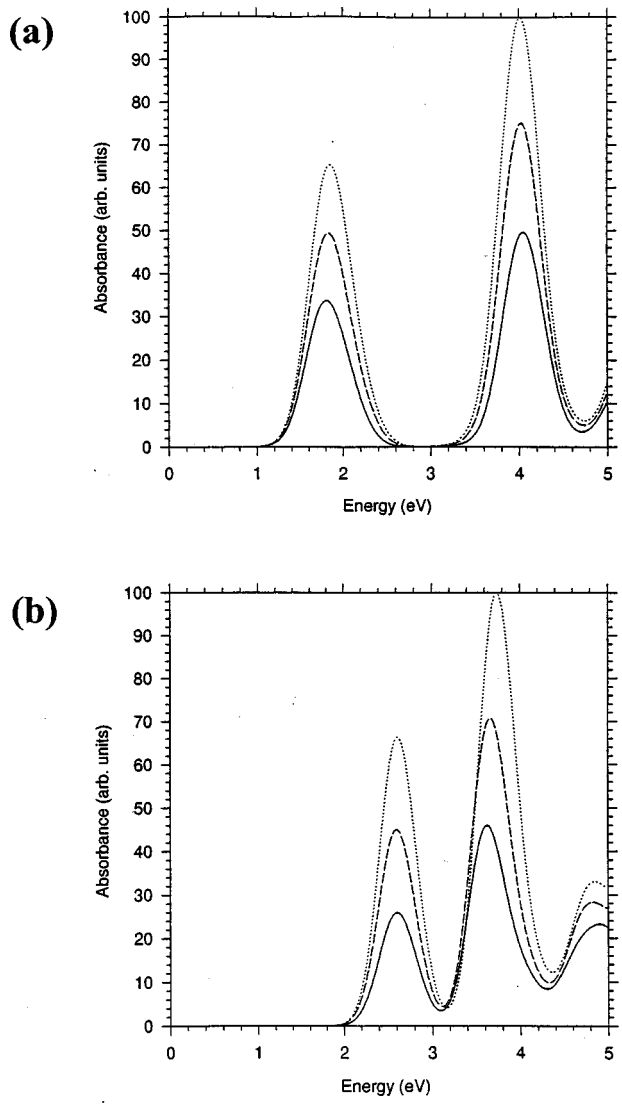

FIG. 9. (a) VEH and (b) INDO/SCI calculated absorption spectra of the PB dimer (solid line), trimer (dashed line), and tetramer (dotted line).

C. Pernigraniline base

1. Geometric structure

Figure 2(c) illustrates the AM1-optimized geometry of the PB unit cell, as extracted from the center of the eight-ring oligomer (tetramer); this repeat unit contains two phenylene rings, one of them ($C1$) presenting a quinoid structure ($C_p-N=1.298$ Å, $C_p-C_0\sim 1.477$ Å, $C_0-C_0=1.340$ Å), while the other ($C2$) is characterized by an aromatic character ($C_p-N=1.409$ Å, $C_p-C_0\sim 1.412$ Å, and $C_0-C_0=1.387$ Å). The quinoid ring hardly leaves the plane defined by the nitrogen atoms ($T=2°$), while the aromatic ring largely goes out of this plane ($T=-58°$). The pernigraniline base therefore presents both bond-length and torsion-angle dimerizations.[30]

2. VEH oligomer calculations

The VEH results indicate that the HOMO of the PB oligomers is systematically localized on aromatic units and displays weaker contributions on adjacent quinoid units; in contrast, the LUMO presents LCAO-π coefficients exclusively on the quinoid units (—N═Q═N—). These trends once again reflect the total breakdown of electron-hole symmetry in polyaniline chains. As for LEB and EB, the VB and CB bands of PB progressively build up with increasing oligomer size [see Fig. 4(c)].

Figure 9(a) presents the VEH absorption spectra of the PB dimer, trimer, and tetramer described in Fig. 1(a). No significant changes in the position and relative intensities of the absorption features are observed with increasing chain length. Two peaks are calculated at 1.85 and 4.01 eV for the tetramer. The first peak corresponds to the superimposition of several features that mainly originate from one-electron transitions between the last four occupied levels and the lowest four unoccupied levels, among which H-1$\rightarrow L$ transition calculated at 1.88 eV is found to dominate in intensity; note that the molecular orbitals involved in the description of this peak are part of the VB and CB bands at the polymer scale [see Fig. 4(c)]. The second feature observed at 4.01 eV corresponds to the overlap of one-electron transitions (in an energy range between 3.8 and 4.1 eV) taking place between occupied molecular orbitals and the lowest three unoccupied levels.

TABLE III. INDO/SCI transition energies, oscillator strengths, and main CI expansion coefficients of the lowest energy absorption features (below 4.5 eV) in the PB oligomers.

Number of rings	Transition energy (eV)	Oscillator strength	Main CI expansion coefficients of the excited states
4	2.59	0.76	$-0.73(H\rightarrow L)-0.29(H-6\rightarrow L)+0.28(H\rightarrow L+1)$
	3.58	0.11	$-0.63(\mathrm{H}-10\rightarrow\mathrm{L}+1)-0.48(\mathrm{H}-10\rightarrow\mathrm{L})$ $-0.32(H-10\rightarrow L+8)$ $-0.25(H-9\rightarrow L+1)$
	3.62	1.29	$0.40(H\rightarrow L)-0.36(H-3\rightarrow L)-0.33(H-6\rightarrow L)$ $+0.23(H-10\rightarrow L+1)+0.22(H-2\rightarrow L+1)$ $-0.22(H-12\rightarrow L)$
	3.98	0.25	$0.41(\mathrm{H}\rightarrow\mathrm{L}+1)-0.33(\mathrm{H}-1\rightarrow\mathrm{L})$ $-0.28(H-9\rightarrow L+1)$ $-0.26(H-3\rightarrow L+1)$
8	2.60	1.91	$-0.56(\mathrm{H}\rightarrow\mathrm{L})-0.44(\mathrm{H}\rightarrow\mathrm{L}+1)$ $+0.23(H-1\rightarrow L+2)$ $+0.23(H-1\rightarrow L)$
	2.72	0.20	$-0.56(\mathrm{H}-1\rightarrow\mathrm{L})-0.31(\mathrm{H}\rightarrow\mathrm{L}+1)$ $+0.30(H-2\rightarrow L+1)$ $+0.28(H\rightarrow L+2)$
	3.71	2.57	$0.29(H-7\rightarrow L)+0.25(H-6\rightarrow L+1)$ $+0.22(H\rightarrow L)$ $-0.22(H-12\rightarrow L+1)-0.21(H-4\rightarrow L+3)$
	3.84	0.59	$-0.28(\mathrm{H}-1\rightarrow\mathrm{L})+0.21(\mathrm{H}-19\rightarrow\mathrm{L}+3)$ $-0.20(H-4\rightarrow L+3)$ $+0.20(H-7\rightarrow L)$
	4.21	0.14	$0.31(\mathrm{H}-1\rightarrow\mathrm{L}+2)-0.23(\mathrm{H}-1\rightarrow\mathrm{L}+3)$ $+0.23(H-2\rightarrow L+2)$ $+0.21(H-6\rightarrow L+2)-0.21(H-19\rightarrow L+1)$

3. INDO/SCI calculations

We report in Table III the nature of the lowest-lying excited states of the PB tetramer and display the associated INDO/SCI simulated spectra in Fig. 9(b). The lowest energy absorption feature of the tetramer (at 2.60 eV) primarily originates from electron transitions from the HOMO to the LUMO and $L+1$ levels. The dominant contribution ($H\rightarrow L$ transition) becomes increasingly contaminated by additional contributions with longer chain lengths, which involve the various levels forming the VB and CB bands in the polymer. The nature of the first transition (measured at 2.3 eV) is very different from that in the EB oligomers, despite the fact that similar electronic configurations are involved; indeed, the PB chains present a chemical structure without amine sites, which therefore prevents the formation of ''charge-transfer'' excitons. The second absorption band of the PB tetramer [at 3.74 eV, Fig. 9(b)], is mainly due to an optical feature calculated at 3.71 eV, corresponding to a large mixing of excitations from occupied levels to the three lowest unoccupied levels (see Table III).

We have also carried out highly sophisticated CI calculations including from singly to fourfold excited configurations. The results do not show contributions arising from double excitations in the description of the optical features below 5.0 eV, in contrast to the theoretical results reported earlier by Sjögren and Stafström.[40]

The plots presented in Fig. 9(b) again illustrate that the position of the absorption peaks are almost unchanged with increasing chain length; indeed, the transition energy of the first peak remains unaffected ($\sim$2.60 eV), while the second band tends to be very slightly blueshifted (from 3.63 eV in the dimer to 3.74 eV in the tetramer) as the chain size is increased. We stress that our results are in close agreement with the experimental absorption spectrum of octa-aniline in the fully oxidized state,[36] where two bands are observed at 2.5 and 4.0 eV. The CI results obtained for the PB tetramer (i.e., three absorption bands at 2.61, 3.74, and 4.85 eV) are also consistent with the experimental values reported for PB chains around 2.3, 3.8, and 4.3 eV.[14,15] Note that the third peak observed in Fig. 9(b) corresponds to a large mixing of configurations and is weakly redshifted with increasing chain length.

4. VEH band structure

Figure 10(a) presents the VEH one-electron band structure of a single PB polymer chain [whose representative unit cell is illustrated in Fig. 2(c)]. Since two π electrons are extracted per unit cell with respect to the LEB chain, the upper branch of the VB band of LEB [see Fig. 5(a)] is emptied to become the CB band of the PB chain; as a result, there is no longer a degeneracy at the end of the Brillouin zone due to the opening of a Peierls gap induced both by torsion-angle and bond-length dimerizations.[30] The resulting

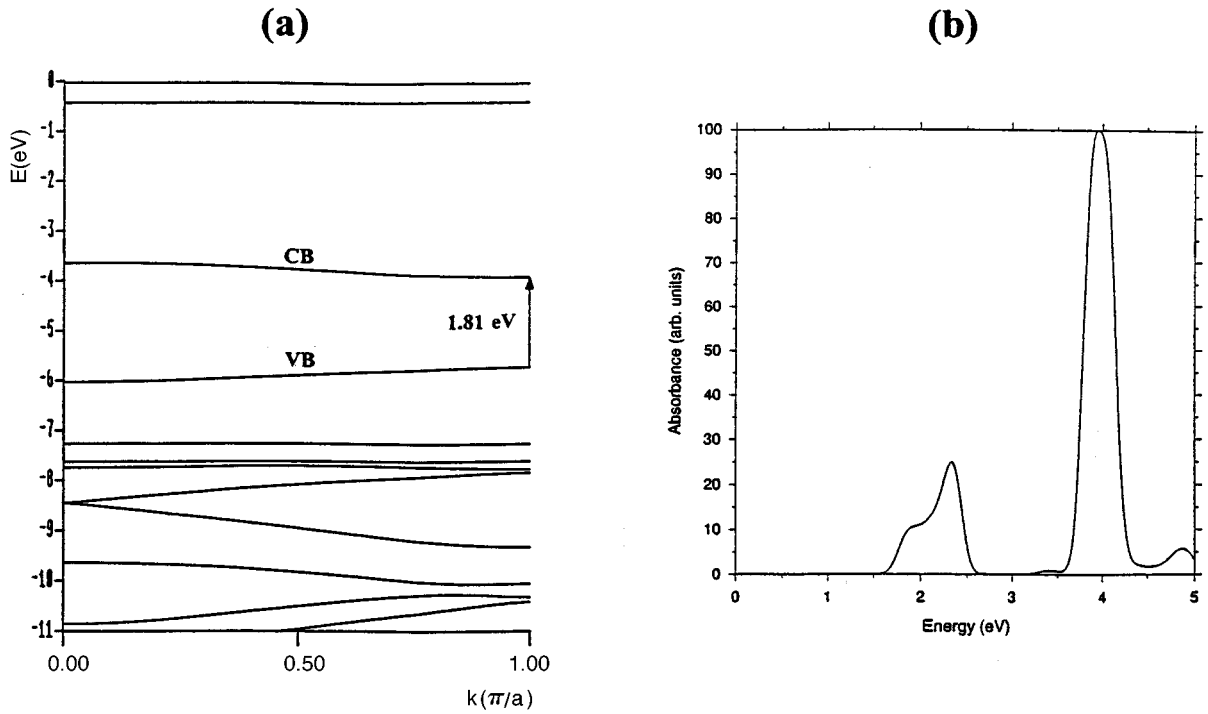

FIG. 10. VEH results relative to a neutral single PB chain: (a) calculated one-electron band structure; (b) associated optical-absorption spectrum.

valence and conduction bands both possess bandwidths on the order of 0.30 eV. It is interesting to note that the ionization potential of PB, corrected for solid-state effects, is estimated at 5.7 eV, i.e., at a value higher than those reported for LEB and EB (4.3 and 4.7 eV, respectively); these trends are fully consistent with the higher degree of oxidation of PB. The electron affinity calculated for PB at -3.9 eV is, however, close to the value obtained for EB at -3.8 eV. The Peierls gap provided by the present VEH calculations is 1.81 eV, this value is in much better agreement with the experimental measurements [lowest energy peak around 2.3 eV with an onset close to 1.7 eV (Refs. 14 and 15)] than previous VEH calculations,[30] due to the use of a refined geometrical description of the polymer unit cell (it is worth stressing that recent UPS measurements[57] once again validate the good description of the PB one-electron structure provided by the VEH formalism).

The VEH absorption spectrum of the PB polymer chain displays a large absorption band in the energy range between 1.7 and 2.5 eV, with a maximum at 2.4 eV and a shoulder at 1.8 eV [see Fig. 10(b)]. This band originates from electronic transitions taking place between the HOMO and LUMO bands. The second absorption band observed around 3.9 eV consists of two distinct features at 3.9 and 4.1 eV; these originate from electronic transitions between the HOMO-2 and HOMO-3 bands to the LUMO band; these merge in the simulated spectrum due to their weak separation. The VEH calculations can thus afford a rationalization for the absorption bands measured at 2.30, 3.80, and 4.30 eV in the experimental spectrum of the PB polymer.[14,15]

The VEH wave functions of the HOMO and LUMO of the PB unit cell are represented in Fig. 6(c), the HOMO (LUMO) is mainly localized on the aromatic (quinoid) rings and adjacent nitrogen atoms, as described for the PB oligomers.

IV. CONCLUSIONS

We have investigated in this work the chain-length dependence of the electronic and optical properties of oligomers representative of the three base forms of polyaniline. Analysis of the AM1-optimized geometry of these oligomers strongly suggests that EB can be viewed as an alternated copolymer of LEB and PB. EB is characterized by a torsion-angle dimerization ($\Delta T = 29°$) that is intermediate between those calculated for LEB ($\Delta T = 0°$) and PB ($\Delta T = 60°$), as a consequence of the presence of quinoid moieties every fourth phenylene ring along the chain. Such a description is further validated by an analysis of the AM1 Mulliken charge distributions and the VEH-calculated ionization potential and electron affinity values showing that EB combines the electronic properties of the LEB and PB base forms.

The INDO/SCI-calculated absorption spectra of neutral oligoanilines representative of the three base forms of polyaniline are in very good agreement with the experimental data reported for oligomers and the corresponding polymers. The correlated calculations show that the optical transitions are weakly modified as a function of chain length, due to a lack of significant π delocalization of the molecular orbitals induced by steric effects and by the incorporation of nitrogen atoms interconnecting the adjacent phenylene rings.

The INDO/SCI results indicate that the lowest energy absorption feature in the leucoemeraldine base primarily originates in electronic transitions between the highest occupied and lowest unoccupied levels, i.e., between the valence and

conduction bands at the polymer scale. In the emeraldine base, we demonstrate that a correlated approach is required to suitably describe the lowest energy peak measured around 2.0 eV. Analysis of the changes occurring in the lowest-lying excited state of emeraldine oligomers shows that a local charge transfer takes place between a quinoid ring (gain of $-1/2\,|e|$) and the adjacent imine/phenyl/amine units (loss of $-1/4\,|e|$ for each) and gives rise to the formation of a confined intramolecular charge-transfer exciton. Despite the fact that the lowest energy absorption occurs at nearly the same energy in EB and PB, the absorption peak has a very different nature in pernigraniline base (and corresponds to a Peierls transition between the valence and conduction bands at the polymer scale). The higher energy features observed around 4 eV in EB and PB oligomers are described by a very large mixing of excitations.

AM1/SCI optimization allows us to take into account the geometric relaxation in the lowest-lying excited state and reveals a slightly different origin of the local charge transfer ($-0.5|e|$) which takes place between the reduced (aromatic/amine sites) and the oxidized units (quinoid/imine sites) of the EB chains.

Our calculations also indicate that the VEH approach is reliable to simulate the absorption spectra of the LEB and PB oligomers and corresponding polymers but fails to reproduce the optical properties of EB; this is due to the one-electron nature of the VEH formalism since a proper description of the lowest excited state of EB requires a correlated approach. On the other hand, the excellent agreement between the VEH one-electron band structures of polyanilines and recent UPS experiments is clear evidence that the occupied levels of the one-electron structure are well-depicted within the VEH formalism.

Finally, we stress that the results of our work illustrate that the oligomer approach is a very useful tool to shed light onto the properties of the polyaniline chains. The oligoanilines can be considered as excellent model systems since there is hardly any significant evolution of the electronic and optical properties as the chain grows.

ACKNOWLEDGMENTS

This work is partly supported by the Belgian Prime Minister Office of Science Policy (SSTC) ''Pôle d'Attraction Interuniversitaire en Chimie Supramoléculaire et Catalyse,'' the Belgian National Fund for Scientific Research (FNRS/FRFC), the Ministère de la Région Wallonne, The European Commission (Human Capital and Mobility Network PANET), and an IBM Academic Joint Study. J. C. received support from the Belgian National Fund for Scientific Research (FNRS).

[1] A. G. MacDiarmid and A. J. Epstein, J. Chem. Soc. Faraday Trans. **88**, 317 (1989).

[2] A. G. MacDiarmid and A. J. Epstein, in *Electrical, Optical and Magnetic Properties of Organic Solid State Materials*, edited by L. Y. Chiang, D. O. Cowan, and P. M. Chaikin MRS Symposia Proceedings No. 173 (Materials Research Society, Pittsburgh, 1990), p. 283.

[3] R. P. Mc Call, J. M. Ginder, J. M. Leng, H. J. Ye, S. K. Manohar, J. G. Masters, G. E. Asturias, A. G. MacDiarmid, and A. J. Epstein, Phys. Rev. B **41**, 5202 (1990).

[4] K. G. Neoh, E. T. Kang, and K. L. Tan, J. Phys. Chem. **96**, 6777 (1992).

[5] Y. Cao, P. Smith, and A. J. Heeger, Synth. Met. **32**, 263 (1989).

[6] J. A. Osaheni, S. A. Jenekhe, H. Vanherszeele, J. S. Meth, Y. Sun, and A. G. MacDiarmid, J. Phys. Chem. **96**, 2830 (1992).

[7] S. Cully, M. C. Petty, and A. P. Monkman, Synth. Met. **55–57**, 183 (1993).

[8] S. Stafström, B. Sjögren, and J. L. Brédas, Synth. Met. **29**, E219 (1989).

[9] C. B. Duke, E. M. Conwell, and A. Paton, Chem. Phys. Lett. **131**, 82 (1986).

[10] Z. G. Soos, D. S. Galvao, and S. Etermad, Adv. Mater. **6**, 280 (1994).

[11] D. Beljonne, Z. Shuai, R. H. Friend, and J. L. Brédas, J. Chem. Phys. **102**, 2042 (1995).

[12] M. C. dos Santos, and J. L. Brédas, Phys. Rev. Lett. **62**, 2499 (1989).

[13] W. P. Su, J. R. Schrieffer, and A. J. Heeger, Phys. Rev. Lett. **42**, 1698 (1979).

[14] J. M. Leng, J. M. Ginder, R. P. Mc Call, H. J. Ye, A. J. Epstein, Y. Sun, S. K. Manohar, and A. G. MacDiarmid, Synth. Met. **41–43**, 1311 (1991); J. M. Leng, R. P. Mc Call, K. R. Cromack, Y. Sun, S. K. Manohar, A. G. MacDiramid, and A. J. Epstein, Phys. Rev. B **48**, 15 719 (1993).

[15] Y. Cao, Synth. Met. **35**, 319 (1990).

[16] J. G. Masters, Y. Sun, A. G. MacDiarmid, and A. J. Epstein, Synth. Met. **41–43**, 715 (1991).

[17] A. G. MacDiarmid and A. J. Epstein, in *Conjugated Polymeric Materials: Opportunities in Electronics, Optoelectronics, and Molecular Electronics*, edited by J. L. Brédas and R. R. Chance NATO-ASI series, Vol. E183 (Kluwer, Dordrecht, 1990), p. 53.

[18] *Conjugated Polymers: The Novel Science and Technology of Highly Conducting and Nonlinear Optically Active Materials*, edited by J. L. Brédas and R. Silbey (Kluwer, Dordrecht, 1991).

[19] J. C. Chiang and A. G. MacDiarmid, Synth. Met. **13**, 193 (1986).

[20] A. G. MacDiarmid, A. F. Richter, and A. J. Epstein, Synth. Met. **18**, 285 (1987).

[21] S. Stafström, J. L. Brédas, A. J. Epstein, H. S. Woo, D. B. Tanner, W. S. Huang, and A. G. MacDiarmid, Phys. Rev. Lett. **59**, 1464 (1987).

[22] A. P. Monkman and P. Adams, Solid State Commun. **78**, 1 (1991).

[23] N. S. Sariciftci, A. J. Heeger, and Y. Cao, Phys. Rev. B **49**, 5988 (1994).

[24] *Intrinsically Conducting Polymers: An Emerging Technology*, edited by M. Aldissi NATO-ASI series, Vol. E246 (Kluwer, Dordrecht, 1992).

[25] J. Miller, Adv. Mater. **5**, 671 (1993).

[26] V. G. Kulkarni, R. Mathew, and J. C. Campbell, Synth. Met. **55–57**, 3780 (1993).

[27] G. Gustafsson, Y. Cao, G. M. Treacy, F. Klavetter, N. Colaneri, and A. J. Heeger, Nature (London) **357**, 477 (1992).

[28] J. M. Ginder and A. J. Epstein, Phys. Rev. B **41**, 10 674 (1990).
[29] J. M. Ginder, A. J. Epstein, and A. G. MacDiarmid, Solid State Commun. **72**, 987 (1989).
[30] J. L. Brédas, C. Quattrocchi, J. Libert, A. G. MacDiarmid, J. M. Ginder, and A. J. Epstein, Phys. Rev. B **44**, 6002 (1991).
[31] J. L. Brédas, in *Proceedings of the Nobel Symposium on Conjugated Polymers and Related Materials: The Interconnection of Chemical and Electronic Structure*, edited by W. R. Salaneck, I. Lundström, and B. Rånby (Oxford University Press, Oxford, 1992), p. 187.
[32] R. P. Mc Call, J. M. Ginder, M. G. Roe, G. E. Asturias, E. M. Scheer, A. G. MacDiarmid, and A. J. Epstein, Phys. Rev. B **39**, 10 174 (1989).
[33] J. M. Leng, J. M. Ginder, R. P. Mc Call, H. J. Ye, Y. Sun, S. K. Manohar, A. G. MacDiarmid, and A. J. Epstein, Phys. Rev. Lett. **68**, 1184 (1992).
[34] R. P. Mc Call, J. M. Ginder, J. M. Leng, K. A. Coplin, H. J. Ye, A. J. Epstein, G. E. Asturias, S. K. Manohar, J. G. Masters, E. M. Scheer, Y. Sun, and A. G. MacDiarmid, Synth. Met. **41–43**, 1329 (1991).
[35] M. Angelopoulos, G. E. Asturias, S. P. Ermer, A. Ray, E. M. Scheer, A. G. MacDiarmid, M. Akhtar, Z. Kiss, and A. J. Epstein, Mol. Cryst. Liq. Cryst. **160**, 151 (1988).
[36] F. L. Lu, F. Wudl, M. Nowak, and A. J. Heeger, J. Am. Chem. Soc. **108**, 8311 (1986).
[37] L. W. Shacklette, J. F. Wolf, S. Gould, and R. H. Baughman, J. Chem. Phys. **88**, 3955 (1988).
[38] A. P. Monkman, D. Bloor, G. C. Stevens, J. C. H. Stevens, and P. Wilson, Synth. Met. **29**, E277 (1989).
[39] S. M. Yang, W. M. Shiah, and J. J. Lai, Synth. Met. **41–43**, 757 (1991).
[40] B. Sjögren and S. Stafström, J. Chem. Phys. **88**, 3840 (1988).
[41] S. Stafström and J. L. Brédas, J. Mol. Struct. **188**, 393 (1989).
[42] J. Libert, J. L. Brédas, and A. J. Epstein, Phys. Rev. B **51**, 5711 (1995).
[43] M. J. S. Dewar, E. G. Zoebish, E. F. Healy, and J. J. P. Stewart, J. Am. Chem. Soc. **107**, 3092 (1985).
[44] M. J. S. Dewar and Y. C. Yuang, Inorg. Chem. **29**, 3881 (1990).
[45] J. P. Pouget, M. E. Jozefowicz, A. J. Epstein, X. Tang, and A. G. MacDiarmid, Macromolecules **24**, 779 (1991).
[46] J. M. André, L. A. Burke, J. Delhalle, G. Nicolas, and Ph. Durand, Int. J. Quantum Chem. Quantum Biol. Symp. **13**, 283 (1979).
[47] J. L. Brédas, R. R. Chance, R. Silbey, G. Nicolas, and Ph. Durand, J. Chem. Phys. **75**, 255 (1981).
[48] M. C. Zerner, G. H. Loew, R. F. Kichner, and U. T. Mueller-Westerhoff, J. Am. Chem. Soc. **102**, 589 (1980).
[49] M. Logdlünd, W. R. Salaneck, F. Meyers, J. L. Brédas, G. A. Arbuckle, R. H. Friend, A. B. Holmes, and G. Froyer, Macromolecules **26**, 3815 (1993).
[50] J. Cornil, D. Beljonne, and J. L. Brédas, J. Chem. Phys. **103**, 834 (1995); **103**, 842 (1995).
[51] J. Guay, P. Kasai, A. Diaz, R. Wu, J. M. Tour, and L. H. Lao, Chem. Mater. **4**, 1097 (1992).
[52] R. Schenk, H. Gregorius, and K. Müllen, Adv. Mater. **3**, 492 (1991).
[53] Z. Shuai, D. Beljonne, and J. L. Brédas, J. Chem. Phys. **97**, 1132 (1992).
[54] H. S. Woo, O. Lhost, S. C. Graham, D. D. C. Bradley, R. H. Friend, C. Quattrocchi, J. L. Brédas, R. Shenk, and K. Müllen, Synth. Met. **59**, 13 (1993).
[55] B. E. Kohler, in *Conjugated Polymers: The Novel Science and Technology of Highly Conducting and Nonlinear Optically Active Materials* (Ref. 18), p. 405.
[56] S. Stafström and B. Sjögren (personal communication).
[57] P. Barta, T. Kugler, W. R. Salaneck, J. L. Brédas, R. Lazzaroni, J. L. Brédas, and A. P. Monkman (unpublished).